MTL TR 87-38

THE EFFECT OF ION IMPLANTATION ON THE CORROSION BEHAVIOR OF A HIGH-DENSITY SINTERED TUNGSTEN ALLOY

FRANK C. CHANG and MILTON LEVY
METALS RESEARCH DIVISION

SIN-SHONG LIN
MATERIALS CHARACTERIZATION DIVISION

August 1987

US ARMY
LABORATORY COMMAND
MATERIALS TECHNOLOGY
LABORATORY

U.S. ARMY MATERIALS TECHNOLOGY LABORATORY
Watertown, Massachusetts 02172-0001

The findings in this report are not to be construed as an official Department of the Army position, unless so designated by other authorized documents.

Mention of any trade names or manufacturers in this report shall not be construed as advertising nor as an official indorsement or approval of such products or companies by the United States Government.

DISPOSITION INSTRUCTIONS

Destroy this report when it is no longer needed.
Do not return it to the originator.

UNCLASSIFIED

SECURITY CLASSIFICATION OF THIS PAGE (When Data Entered)

REPORT DOCUMENTATION PAGE	READ INSTRUCTIONS BEFORE COMPLETING FORM
1. REPORT NUMBER: MTL TR 87-38	2. GOVT ACCESSION NO.: ADA185713
3. RECIPIENT'S CATALOG NUMBER	
4. TITLE (and Subtitle): THE EFFECT OF ION IMPLANTATION ON THE CORROSION BEHAVIOR OF A HIGH-DENSITY SINTERED TUNGSTEN ALLOY	5. TYPE OF REPORT & PERIOD COVERED
	6. PERFORMING ORG. REPORT NUMBER
7. AUTHOR(s): Frank C. Chang, Milton Levy, and Sin-Shong Lin	8. CONTRACT OR GRANT NUMBER(s)
9. PERFORMING ORGANIZATION NAME AND ADDRESS: U.S. Army Materials Technology Laboratory, Watertown, Massachusetts 02172-0001, ATTN: SLCMT-MRD	10. PROGRAM ELEMENT, PROJECT, TASK AREA & WORK UNIT NUMBERS
11. CONTROLLING OFFICE NAME AND ADDRESS: U.S. Army Laboratory Command, 2800 Powder Mill Road, Adelphi, Maryland 20783-1145	12. REPORT DATE: August 1987
	13. NUMBER OF PAGES: 12
14. MONITORING AGENCY NAME & ADDRESS (if different from Controlling Office)	15. SECURITY CLASS. (of this report): Unclassified
	15a. DECLASSIFICATION/DOWNGRADING SCHEDULE

16. DISTRIBUTION STATEMENT (of this Report)

Approved for public release; distribution unlimited.

17. DISTRIBUTION STATEMENT (of the abstract entered in Block 20, if different from Report)

18. SUPPLEMENTARY NOTES

Published in Electrochemical Techniques for Corrosion Engineering, 1986, p.173 to 182.

19. KEY WORDS (Continue on reverse side if necessary and identify by block number)

Corrosion resistance
Tungsten alloys
Density
Ion implantation
Auger electron spectroscopy
Electrochemical tests
Polarization measurement

20. ABSTRACT (Continue on reverse side if necessary and identify by block number)

(SEE REVERSE SIDE)

DD FORM 1 JAN 73 1473 EDITION OF 1 NOV 65 IS OBSOLETE

UNCLASSIFIED

SECURITY CLASSIFICATION OF THIS PAGE (When Data Entered)

Block No. 20

ABSTRACT

The effect of Cr, Ni, Ta, and Ti ion implantation at a dose rate of 2×10^{17} ions cm^{-2} on the electrochemical corrosion behavior of a high density sintered tungsten alloy has been investigated in Cl^- -free and Cl^- containing aqueous solution buffered to pH values of 4, 9, and 12. A three-sweep potentiodynamic polarization technique was used to compare the polarization behavior of unimplanted and implanted surfaces. The surfaces of the ion-implanted tungsten alloy were characterized by Auger electron spectroscopic (AES) analysis.

The Effect of Ion Implantation on the Corrosion Behavior of a High-Density Sintered Tungsten Alloy

F. C. CHANG, M. LEVY, S. S. LIN*

Abstract

The effect of Cr, Ni, Ta, and Ti ion implantation at a dose rate of 2×10^{17} ions cm^{-2} on the electrochemical corrosion behavior of a high-density sintered tungsten alloy has been investigated in Cl^--free and Cl^--containing aqueous solution buffered to pH values of 4, 9, and 12. A three-sweep potentiodynamic polarization technique was used to compare the polarization behavior of unimplanted and implanted surfaces. The surfaces of the ion-implanted tungsten alloy were characterized by Auger electron spectroscopic (AES) analysis.

Introduction

Sintered tungsten alloys are candidate materials for certain US Army applications because of their high density. Until recently, the corrosion of tungsten alloys has not been considered a problem. Andrew, *et al.*,[1] reported that a 90 W, 7.5 Ni, 2.5 Co alloy readily corrodes when exposed to air-saturated water vapor. The authors in a previous paper[2] showed that a tungsten alloy 97.1 W, 1.6 Ni, 0.7 Fe, 0.5 Cu, 0.1 Co also undergoes corrosion when exposed to a chloride-containing aqueous solution. Some dissolution of the tungsten grains and localized attack of the matrix alloy were observed.[2] This paper reports on the effects of Cr, Ni, Ti, and Ta implantation on the corrosion behavior of a sintered tungsten alloy in aqueous solutions of varying pH values by electrochemical techniques.

Experimental Procedure

The sintered tungsten alloy (W2) was fabricated using powder metallurgy techniques (isostatic compaction of mixed metal powders followed by sintering in hydrogen). The basic tungsten content was 97.1%. The matrix composition included 0.7% Fe, 1.6% Ni, 0.1% Co, and 0.5% Cu. Figure 1 is a micrograph of the alloy showing rounded tungsten particles surrounded by a layer of matrix solid solution. Note the porosity in both the tungsten grains and the matrix alloy.

Specimens for electrochemical tests were flat discs, 5/8 in. (16 mm) in diameter and 1/8 in. (3.2 mm) thick. The exposed surface area was 1 cm^2. The specimens were ground to a 64 root mean square (rms) finish, rinsed with distilled water, acetone-degreased, air dried, and ion implanted.

The aqueous solutions used for electrochemical tests were buffered to pH values of 4, 9, and 12 with and without 0.1 molar (M) NaCl. They were prepared from laboratory reagent chemicals and distilled H_2O. The buffers used to fix the pH included citric acid, disodium phosphate, sodium hydrogen carbonate, and sodium hydroxide.

Electrochemical polarization measurements were made utilizing a three-sweep method of potentiodynamic polarization. Prior to sweeping the potential, the specimen was allowed to remain in the solution for at least 30 minutes to permit the potential to come to a steady-state corrosion potential. The three-sweep method involved a positive direction sweep from the corrosion potential to +1.6 V vs SCE. This was followed by a negative direction sweep to a potential 250 mV more negative than the corrosion potential. Finally, there was a second positive direction sweep to a potential of +1.6 V vs SCE. The sweep rate used was 4 V/h throughout. Polarization runs

*Army Materials and Mechanics Research Center, Watertown, Massachusetts.

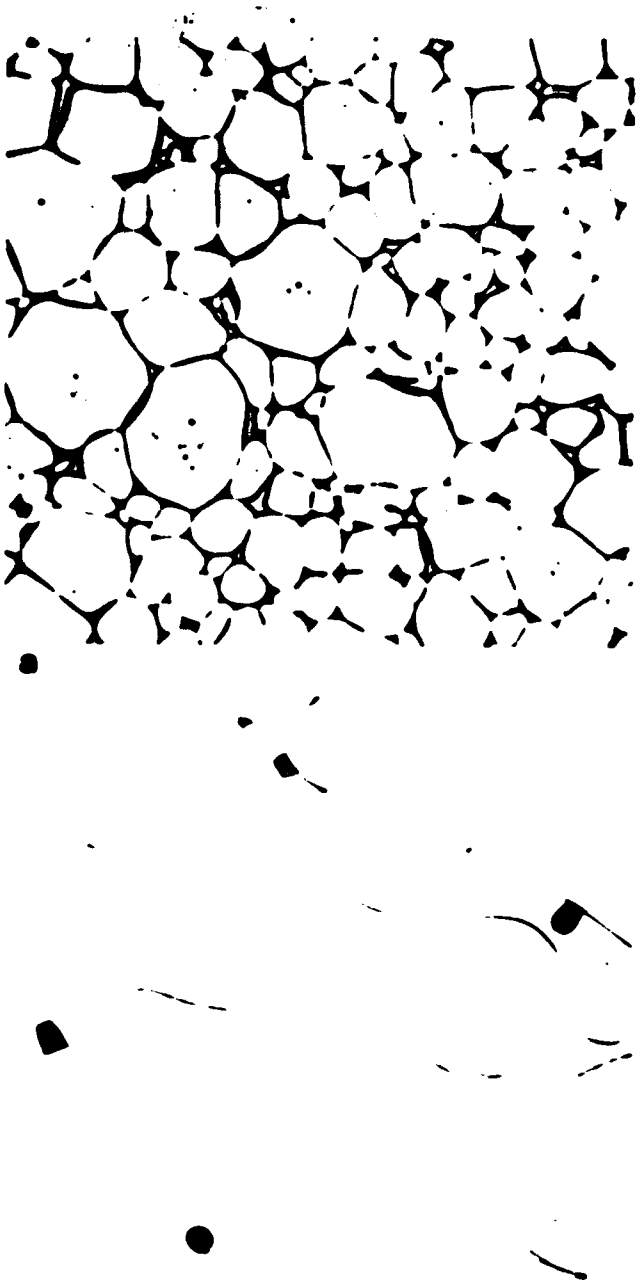

FIGURE 1 – Typical microstructure of the W2 tungsten alloy, unetched, showing porosity: (a) in the grain at 100X and (b) in the matrix at 500X.

were made with the tungsten alloy in both the virgin and ion-implanted conditions in argon purged solutions.

The ion implantation[1] was performed at a dose rate of 2×10^{17} ions cm^{-2}. The energy of singly charged positive ions used varied with the ion implanted: 156 KeV for Cr; 165 KeV for Ni; 160 KeV for Ta; and 142 KeV for Ti. The ion-implanted tungsten alloy specimens were analyzed with an ESCA/Auger instrument and scanning Auger microprobe (SAM) attachment before and after the polarization tests.

[1]Performed by the Naval Research Laboratory, Washington, DC.

The surfaces to be examined were carefully chosen so that the analysis was not made on cracks or depressions. Before the depth profile analysis was performed, the surface topology was examined and then an Auger electron spectrum was taken. From the spectrum, the surface elements and their concentrations could be obtained. The depth profile analyses were made at a minimum of two locations of the specimen surface. The variations of those implanted elements, plus tungsten, oxygen, and carbon and nitrogen signals along the depth were monitored throughout a sputtering period of from 20 to 100 minutes. The ion sputtering was continued until a steady-state signal of tungsten was obtained. The peak heights were then converted to the atomic concentrations using the available sensitivity factors.

Results and Discussion

Unimplanted W2 in Cl-Free Solutions – Effect of pH

The complete, three-sweep potentiodynamic polarization curves for the unimplanted tungsten alloy in aqueous solutions of pH values of 4, 9, and 12 are shown in Figure 2. In the pH 4 solution during the first positive direction sweep, the air-formed oxide film is repaired and replaced above 0.500 V by nonsteady-state film growth and a consequent increase in the anodic current density from ~50 $\mu a/cm^2$ to ~1000 $\mu a/cm^2$. A relatively well-marked hysteresis loop is observed upon a reversal of the sweep direction. Anodic current densities are substantially greater at corresponding potentials in the potential range between 0.500 and 1.400 V. It is believed that the hysteresis loop is attributable to crevice corrosion since crevice attack was observed near the masked surfaces and some porosity was present in the virgin W alloy (both in tungsten grains and in the matrix alloy) (Figure 3). Similar hysteresis loops have been reported for specimens containing synthetic crevices.[3,4] The major difference in the second positive direction sweep is the appearance of an anodic current density peak at ~0.500 V which must be due to an alloying element in the matrix material.

Three-sweep curves for the alloy in the pH 9 solution are similar to each other. They exhibit an active/passive transition at ~ −0.280 V and a secondary peak at ~ +0.200 V. A transpassive region is observed at ~1.400 V. There is no apparent hysteresis loop during the reverse sweep. Again, the three-sweep curves for the alloy in solution of pH 12 are essentially identical to one another. The anodic current density increases to ~560 $\mu a/cm^2$ where it remains fairly constant throughout the potential range −0.250 to 1.140 V, showing that the oxide film remains essentially unchanged. In general, increasing the pH from 4 to 9 to 12 serves to shift the corrosion potential in the more active or electronegative direction. The greatest shift is observed upon increasing the pH from 4 to 9, where the corrosion potential becomes ~330 mV more negative. According to the Pourbaix diagram for tungsten,[5] the passivation area ranges from pH 0 to pH 4 from the corrosion potential and above, to

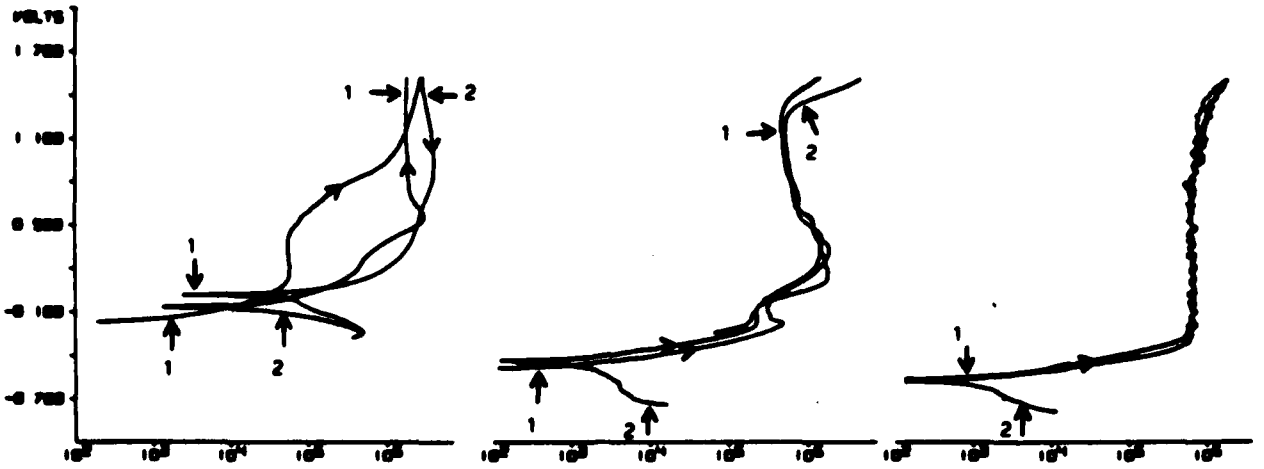

a b c

FIGURE 2 – Polarization curves of W2 in pH of (a) 4, (b) 9, and (c) 12 solutions without chloride.

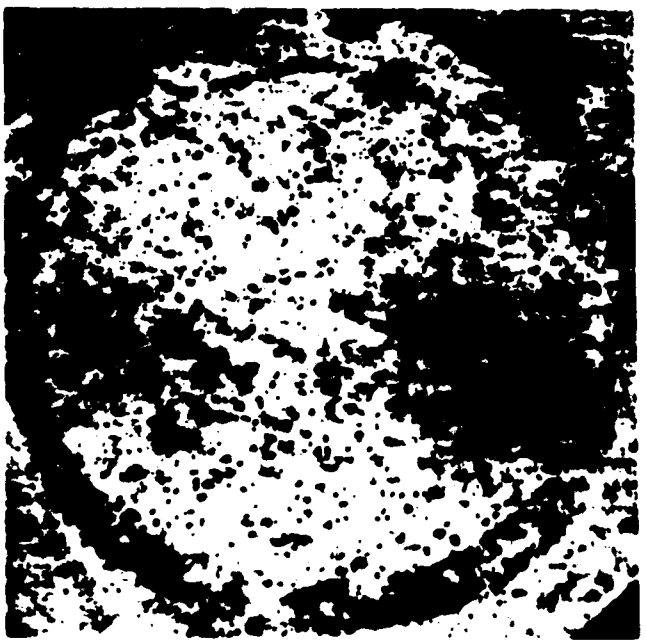

FIGURE 3 – Surface of W2 alloy after polarization scans showing crevice corrosion.

1.4 V where the tungsten is covered by WO_2 or higher oxides WO_3, W_2O_5. The corrosion area extends from the corrosion potential to ~ 1.4 V and above, at pH 4 to 16, and in the more alkaline solutions it has a slight tendency to decompose H_2O with evolution of H_2O dissolving as tungstic ions WO_4^{-2}. In addition, the curves at higher pH exhibit reversibility whereas the curve at pH 4 exhibits a marked hysteresis loop.

Chloride-Free Environment – Chromium-Implanted W2 Alloy

The potentiodynamic polarization curves for the W2 alloy implanted with 2×10^{17} Cr^+ ions cm^{-2} are shown in Figure 4. In this case, there are differences between the first positive sweep for Cr-implanted W2 and the corresponding sweep for unimplanted W2 at pH 4 and 9. At pH 4, the Cr-implanted W2 alloy is more difficult to passivate and the anodic current density is greater throughout the entire potential range. In solution of pH 9, however, the Cr-implanted alloy is more easily passivated while the anodic current density increases at potentials above 0.80 V. These data are consistent with the theoretical Pourbaix diagram for chromium,[5] considering $Cr(OH)_3$ or Cr_2O_3 in solutions not containing chloride. According to the Pourbaix diagram, chromium should be corroding in solution of pH 4 throughout the potential range of the first positive sweep. But at pH 9, passivation is indicated, except at corrosion potentials above 0.80 V where corrosion occurs. The films formed on Cr-implanted W in the pH 9 solution may be slightly more protective than those formed on the unimplanted W2. In solutions of pH 12, the shape of the curves for both the implanted and unimplanted alloy is essentially the same, indicating that the implanted specimen shows no change in the film by the process or the chromium.

Nickel-Implanted W2 Alloy

Figure 5 shows the potentiodynamic polarization curves for Ni-implanted W2 alloy. The curves for both the unimplanted and implanted material have similar shapes, but the anodic current density for the implanted alloy is greater throughout the entire potential range of the sweeps. The main area of corrosion from the Pourbaix diagram lies between pH – 2 and 9. Also, a small area of passivation exists in the pH range of from 9 to 12. Therefore, the implanted Ni provides no beneficial modification of the oxide film throughout the pH range of 4 to 12.

Titanium-Implanted W2 Alloy

The potentiodynamic curves for the W alloy implanted with 2×10^{17} Ti^+ ions cm^{-2} (Figure 6) are similar to corresponding curves for unimplanted W. But in solu-

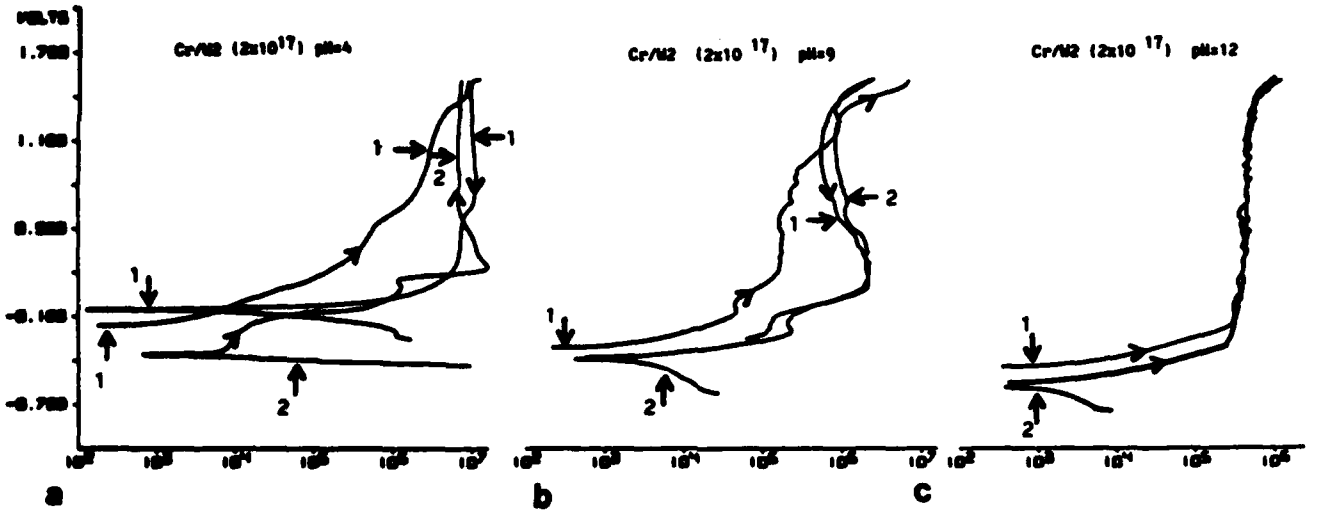

FIGURE 4 – Polarization curves of Cr-implanted W2 in pH of: (a) 4, (b) 9, and (c) 12 solutions without chloride.

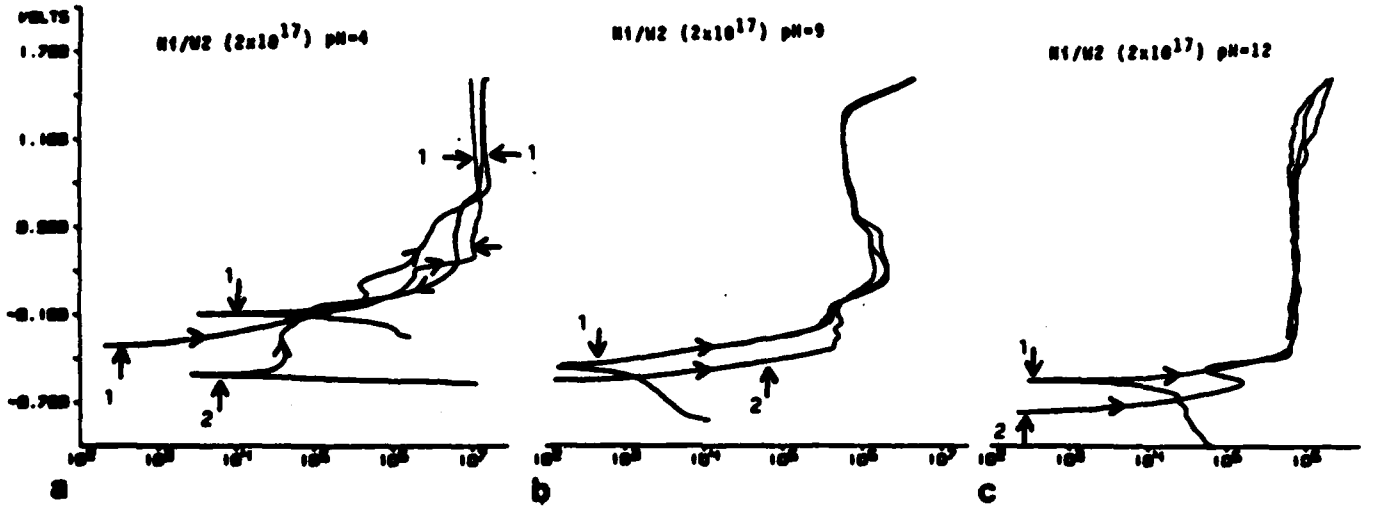

FIGURE 5 – Polarization curves of Ni-implanted W2 in pH of: (a) 4, (b) 9, and (c) 12 solutions without chloride.

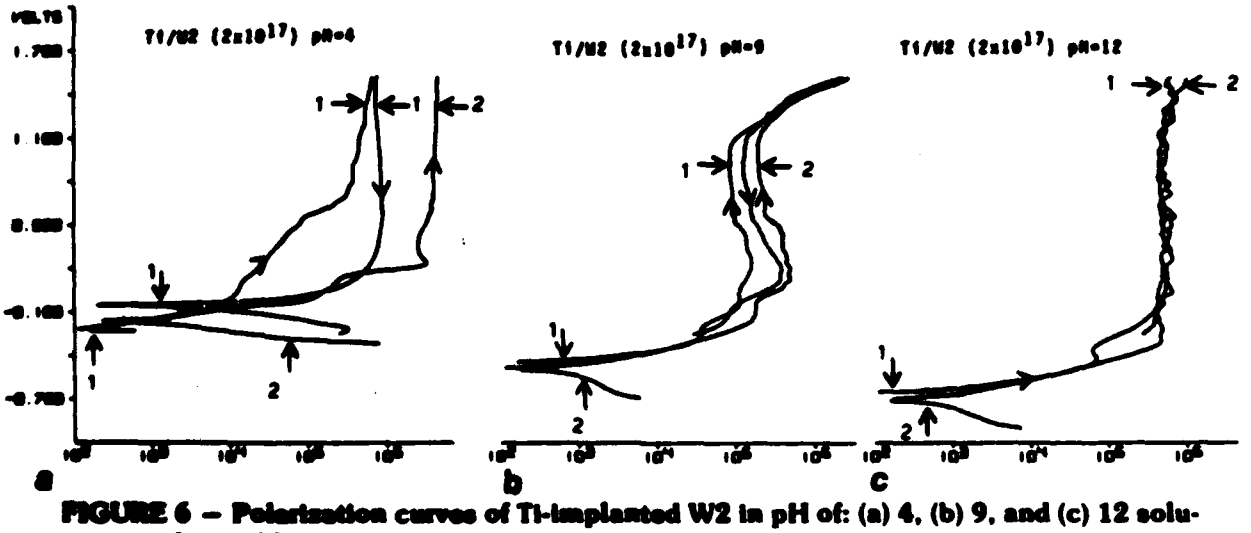

FIGURE 6 – Polarization curves of Ti-implanted W2 in pH of: (a) 4, (b) 9, and (c) 12 solutions without chloride.

FIGURE 7 – Surface of Ti-implanted W2 after exposure to potentiodynamic polarization scans in the pH 9 solution without chloride showing oxide film. (7X)

tions of pH 9 and 12, the magnitude of the anodic current density throughout the potential range of the sweeps is reduced by the implanted species, indicating that the films formed on Ti-implanted W are more protective than those formed on unimplanted W. (See Figure 7.)

Tantalum-Implanted W2 Alloy

Figure 8 shows polarization curves for the Ta-implanted tungsten alloy in solutions of pH values of 4, 9, and 12. The shapes of the curves are similar to those of the unimplanted alloy. The first positive direction sweep with the Ta-implanted alloy in the pH 4 solution is very similar to that observed with the unimplanted alloy. However, the second positive direction sweep in this figure differs from that observed with the unimplanted W alloy in that the current density of the implanted alloy is an order of magnitude greater. According to the Pourbaix diagram, Ta_2O_5, a stable protective oxide, is formed in aqueous solutions of the pH range of from 0 to 14. Nevertheless, larger currents were observed for the implanted alloy. This may be due to the high densities of the elements involved (W alloy ~19.3 g/cm^3, Ta-13.6 g/cm^3) and the magnitude of the ion energy (160 KeV) employed for implantation, which resulted in very low concentrations of Ta on the surface to a depth of 140 A. Tantalum implantation had little or no effect on the polarization curves for the alloy in the pH 9 and 12 solutions.

Unimplanted W2 in Chloride-Containing Solution—Effect of Cl and pH

The complete, three-sweep potentiodynamic polarization curves characteristic of unimplanted W2 alloy in 0.1 M NaCl solution buffered to pH values of 4, 9, and 12 are shown in Figure 9. These curves differ from the corresponding curves in a chloride-free environment as follows: the corrosion potentials are slightly more active, except at pH 9 where they are essentially identical; the passive current densities are markedly greater, and hysteresis loops are observed at all pH values. Increasing the pH increases the anodic current density, particularly from pH 4 to 9.

Cl-Containing Solution—Cr-Implanted W2 Alloy

Figure 10 shows the potentiodynamic polarization curves for Cr-implanted W2 alloy in the pH 4, 9, and 12 solutions. The general shapes of these curves are similar to the curves for the unimplanted alloy. The corrosion potentials remain essentially the same. In solutions of pH

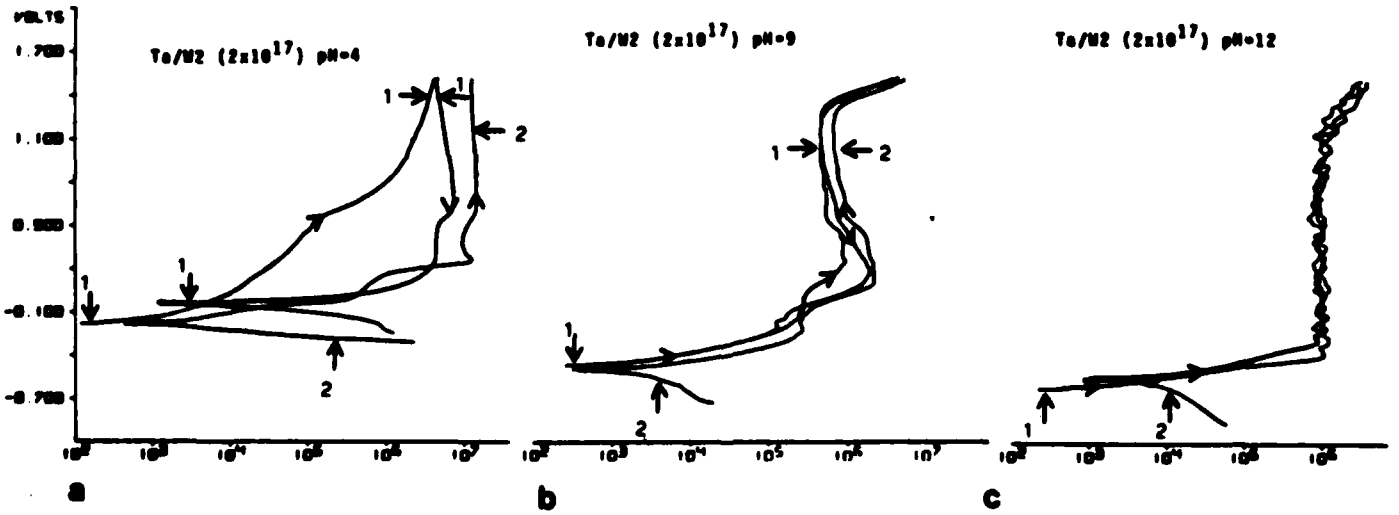

FIGURE 8 – Polarization curves of Ta-implanted W2 in pH of: (a) 4, (b) 9, and (c) 12 solutions without chloride.

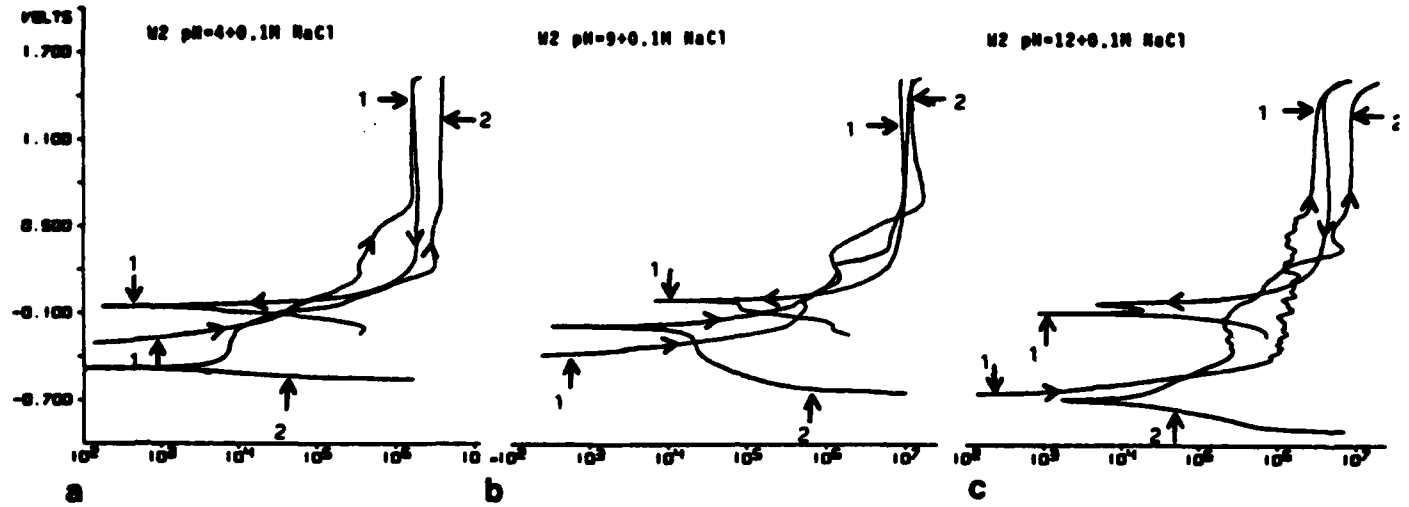

FIGURE 9 – Polarization curves of W2 in pH of: (a) 4, (b) 9, and (c) 12 solutions with chloride.

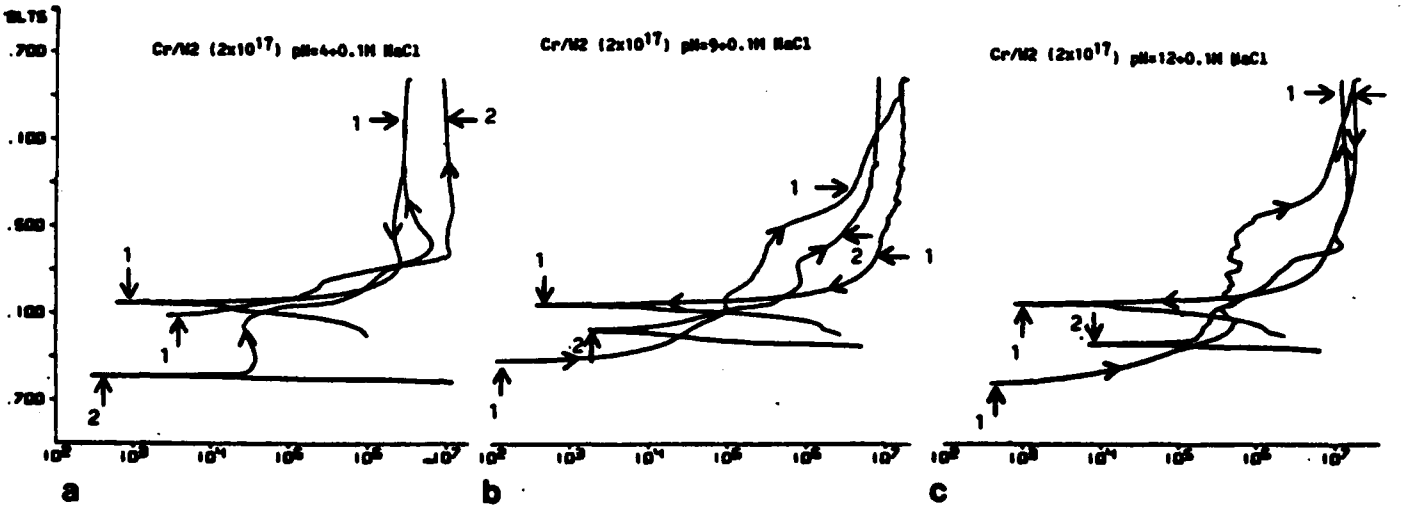

FIGURE 10 – Polarization curves of Cr-implanted W2 in pH of: (a) 4, (b) 9, and (c) 12 solutions with chloride.

4 and 12, the anodic current density for the implanted alloy is larger than that for the unimplanted alloy. At pH 9, however, Cr reduces the anodic current density. These results are consistent with the Pourbaix diagram for chromium in solutions containing chloride and considering $Cr(OH)_3 \cdot nH_2O$ as the stable species. There is a relatively narrow region of passivity in the pH range of 8 to 9 in Cl-containing solutions.

Nickel-Implanted W2 Alloy

Figure 11 shows the potentiodynamic polarization curves for Ni-implanted W alloy in chloride-containing solutions of pH values of 4, 9, and 12. The electrochemical behavior of the Ni-implanted alloy was quite similar to that of the Cr-implanted alloy previously described. The Ni implantation provided a beneficial effect in the pH 9 solution, but produced higher anodic currents in the pH 4 and 12 solutions. Again, results were consistent with the Pourbaix diagram.

Titanium-Implanted W2 Alloy

The potentiodynamic polarization curves for the Ti-implanted alloy in chloride solutions of pH 4, 9, and 12 are shown in Figure 12. In general, the shapes of the curves are similar to those of the unimplanted alloy. But more noble corrosion potentials and smaller currents are observed for the implanted alloy. The hysteresis loops observed in the reverse scans are broader than those observed in similar scans for the unimplanted alloy. In summary, the Ti implantation appears to have a beneficial effect on the alloy, especially in the pH 9 solution.

Ta-Implanted W2 Alloy

The potentiodynamic polarization curves for Ta-implanted W2 alloy are very similar in shape to those for the unimplanted alloy in Cl-containing solution as shown in Figure 13. The beneficial effects of the Ta-implantation are reflected in the smaller anodic currents at potentials up to +0.500 V in the pH 4 solution and to +1.400 V in the pH 9 solution.

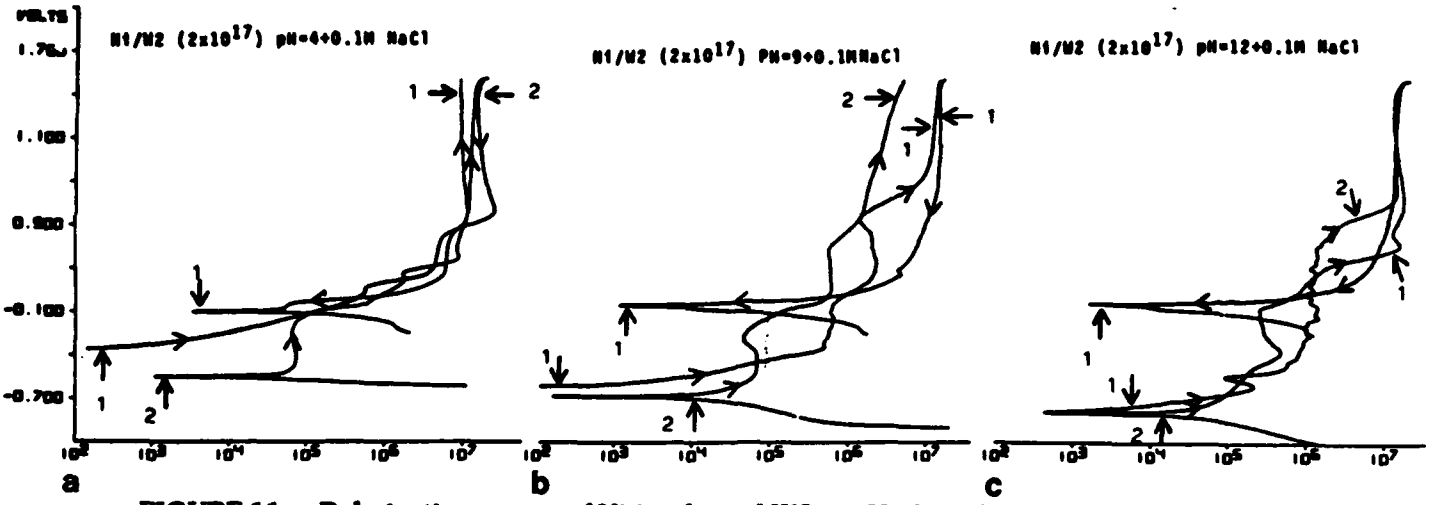

FIGURE 11 – Polarization curves of Ni-implanted W2 in pH of: (a) 4, (b) 9, and (c) 12 solutions with chloride.

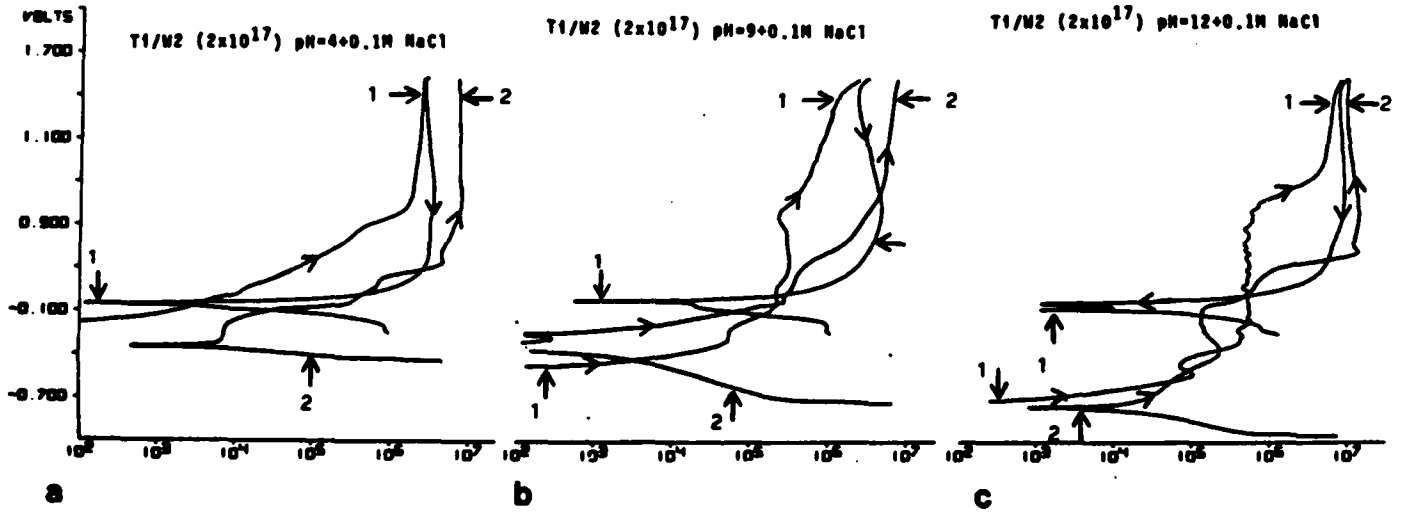

FIGURE 12 – Polarization curves of Ti-implanted W2 in pH of: (a) 4, (b) 9, and (c) 12 solutions with chloride.

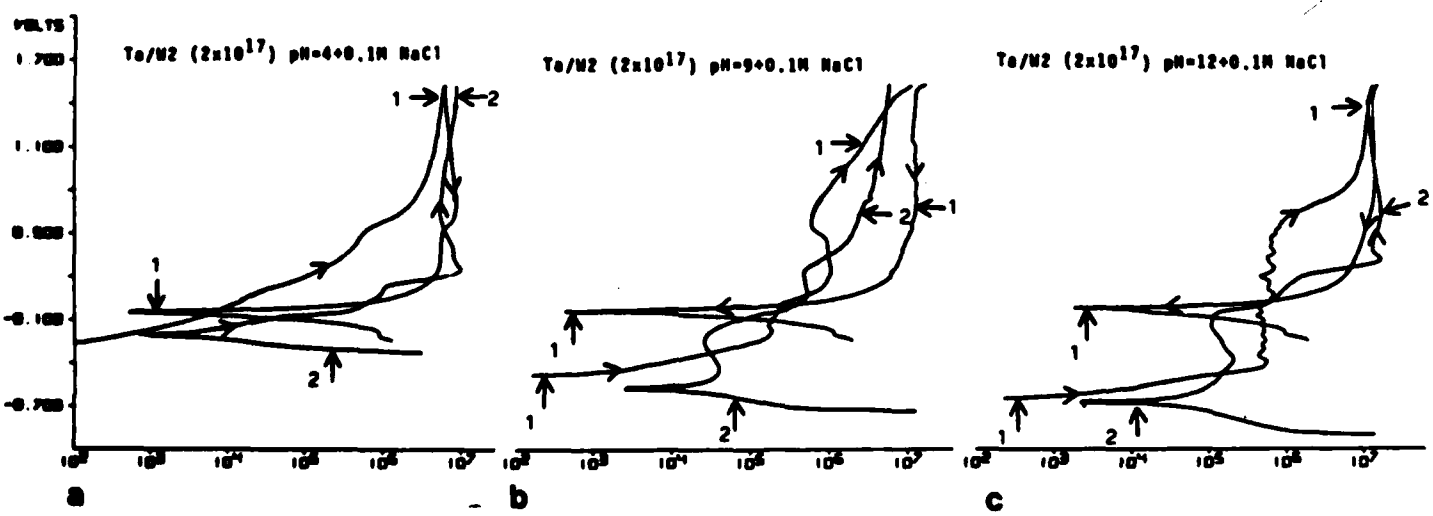

FIGURE 13 – Polarization curves of Ta-implanted W2 in pH of: (a) 4, (b) 9, and (c) 12 solutions with chloride.

TABLE 1 – Summary of Ion-Implanted W2 After Polarization Tests

Specimen Ion/W2-P (pH)-X (salt)	Surface Condition	Elements on Surface Other Than W, C, N, O, & Na (salt) Before DP Analyses (s) = Strong Signal	Depth Profile Analyses: Implanted Ion Width (μm) Error 10%	Depth Profile Analyses: Oxide Thickness Width (μm) Error 10%
W2P4	smooth	Ni, Fe		less than 0.05
W2P9	smooth	Ni, Fe		less than 0.01
W2P12	smooth	Ni, Fe		less than 0.05
W2P4X	deposits	Ni(s), Fe		more than 0.15
W2P9X	deposits	Ni(s), Fe		more than 1
W2P12X	deposits	Fe, Ni		more than 0.4
Ti/W2P4	smooth	Ni	0.12 & shift	less than 0.02
Ti/W2P9	smooth	Ti, Ni, Fe	0.1	less than 0.02
Ti/W2P12	smooth	Ti(s), Ni, Fe	0.12 & shift	more than 0.18
Ti/W2P4X	smooth	Ti(s), Ni, Fe	0.1 & shift	less than 0.02
Ti/W2P9X	deposits	Ti, Ni, Fe	0.12 & shift	about 0.1
Ti/W2P12X	deposits	Ti(s), Ni, Fe	0.13 & shift	about 0.15
Ni/W2P4	smooth	Ni(s), Fe	less than 0.03	less than 0.02
Ni/W2P9	smooth	Ni(s), Fe	0.08	about 0.03
Ni/W2P12	smooth	Ni(s), Fe	about 0.08	about 0.08
Ni/W2P4X	smooth	Ni(s), Fe	more than 0.08	less than 0.02
Ni/W2P9X	smooth	Ni, Fe	about 0.03	more than 0.15
Ni/W2P12X	deposits	Ni, Fe	less than 0.02	more than 0.1
Cr/W2P4	smooth	Cr, Ni	small Cr profile width 0.05	more than 0.1
Cr/W2P9	smooth	Ni, Fe	less than 0.01 extended Ni depth	more than 0.05
Cr/W2P12	coating	Cr, Fe, Ni	less than 0.01	about 0.05
Cr/W2P4X	smooth	Cr, Ni	small Cr profile width 0.05	more than 0.1
Cr/W2P9X	scales, layers	Ni, Fe	null	more than 1
Cr/W2P12X	coatings	Cr, Ni, Fe(s)	less than 0.05	more than 0.2
Ta/W2P4	smooth	Ni, Fe	trace	none
Ta/W2P9	smooth	Ni	trace	more than 0.04
Ta/W2P12	smooth	Ni	trace	about 0.03
Ta/W2P4X	spotty pits	Ni, Fe	trace	less than 0.01
Ta/W2P9X	scales coatings	Ni, Fe	trace extended Ni depth	more than 0.6
Ta/W2P12X	spotty layers	Fe(s), Ni	none	about 0.2

Auger Analysis

The results of Auger analyses of reacted specimens are contained in Table 1 and summarized below.

Unimplanted W2 Alloy

After the potentiodynamic polarization scans, the surfaces of all specimens were enriched with the matrix elements of the W2 alloy, Ni, and Fe. The amounts of Ni and Fe on the surface increased in the chloride-containing solutions. The depth profile analyses showed that anodic oxide films of varying thickness were present on all specimens. The oxide thickness varied widely from a minimum in the chloride-free pH 9 solution to a maximum of 1 μm in the pH 9 chloride solution. In the pH 9 chloride solution, two layers of Ni and W oxide films were found. The nickel film was present on top of the tungsten oxide layer, and it displayed a Gaussian depth profile distribution. In general, thicker anodic oxide films were produced in chloride solutions. It is likely that Cl ions contributed to the accelerated oxide formation.

Ti-Implanted W2 Alloy

The depth profile for titanium before and after polarization runs was similar. Although there were varying degrees of oxide formation as indicated by the oxygen profile curves, the magnitude of the titanium signal in these oxide layers was not changed appreciably and the widths of the profile remained the same (about 0.1 μm). (See Figure 14.) In some instances, a large concentration of titanium was observed on the surface. This was probably due to the displacement of the Ti toward the surface. The Ni and Fe matrix elements also concentrated on the

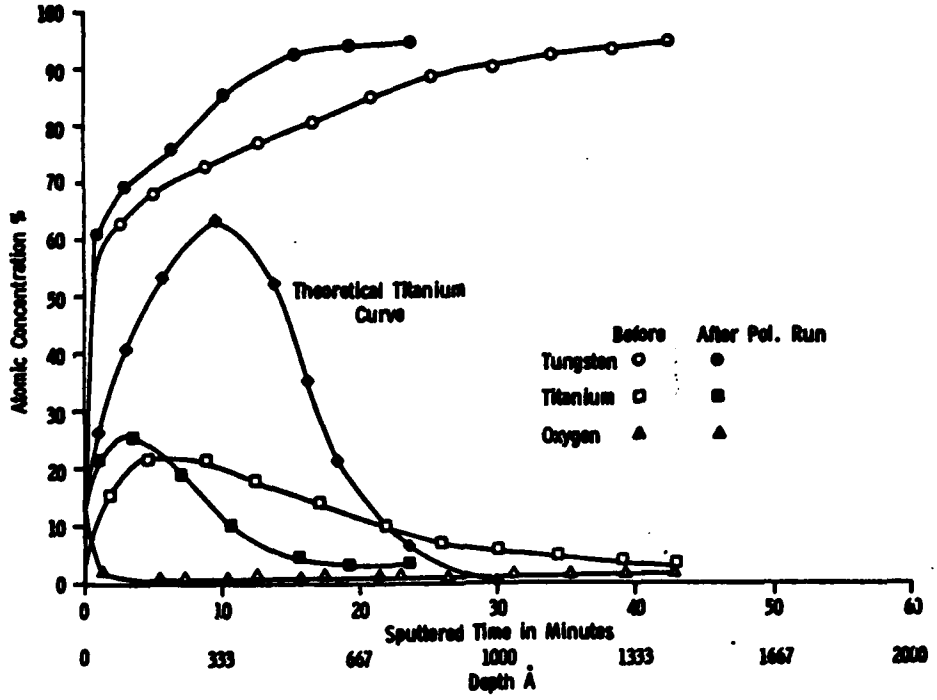

FIGURE 14 – Auger concentration depth profiles of Ti, W, and O before and after Ti-implanted W2 subjected to potentiodynamic polarization in pH 9 solution without chloride. Note the difference between the theoretical and actual profile of Ti.

top surfaces, and the enrichment of these metals on the surface was accelerated in chloride solutions.

Ni-Implanted W2 Alloy

The Ni-implanted W2 was unique in that the metal tended to accumulate on the surface. A high concentration of Ni on the surface was usually observed. The depth profile was found to alter considerably after polarization. In the Cl-free solutions, Ni was displaced significantly toward the surface so that only a portion remained. But in chloride solution, Ni disappeared. A significant oxide layer formation was observed as pH increased in Cl solutions. In the absence of Cl, the widths of the oxygen profile appeared to be associated with those of the nickel profile, that is, a nickel oxide had formed. But in the Cl solution (except for pH 9), the oxygen profile far exceeded that of nickel; that is, other oxides had formed.

Cr-Implanted W2 Alloy

The behavior of the ion-implanted Cr varied widely from solution to solution. The majority of Cr was found to concentrate near or at the surface together with Ni and Fe. The surface topology changed markedly in the high pH solutions with the formation of various oxide layers. In the Cl-free pH 9 solution, the formation of a Ni oxide layer was observed. Although small amounts of Cr, represented by a narrow profile width and a low concentration, were detected in the low pH solutions, no Cr was detected in the high pH Cl solutions.

Ta-Implanted W2 Alloy

Most of the Ta in the implanted surface was lost after the polarization runs (Figure 15). Even in the less corrosive, Cl-free solutions, the Ta profile had nearly disappeared, and the formation of Fe and Ni oxide layers predominated in Cl solutions.

An assessment of corrosion behavior based solely on Auger analyses (depth profile, thickness of oxide layer, distribution of W, and the matrix elements of the alloy) indicates that: (1) generally, corrosion increases with increasing pH and with the addition of Cl and (2) among the implanted species, Ti provides the best protection.

Conclusions

In brief summary, the unimplanted and implanted tungsten alloy exhibits an active/passive transition in the solutions studied, but the magnitude of the passive current density exceeded 100 $\mu a/cm^2$ in most cases. Generally, corrosion rates increase with increasing pH and in the presence of chloride ions. The hysteresis loops observed during reverse sweeps are attributed to crevice corrosion and porosity in both the tungsten grains and the matrix alloy. Among the Cr, Ni, Ta, and Ti implantations, Ti improved the corrosion resistance of the tungsten alloy. The magnitude of the current density throughout the potential range of the sweeps was reduced. The Auger depth profile for titanium before and after potentiodynamic polarization sweeps was similar; i.e., the magnitude of the titanium signal in the oxide layers and the width of the profile remained essentially the same. Generally, Pourbaix diagram data and Auger analysis results were in agreement with the electrochemical data.

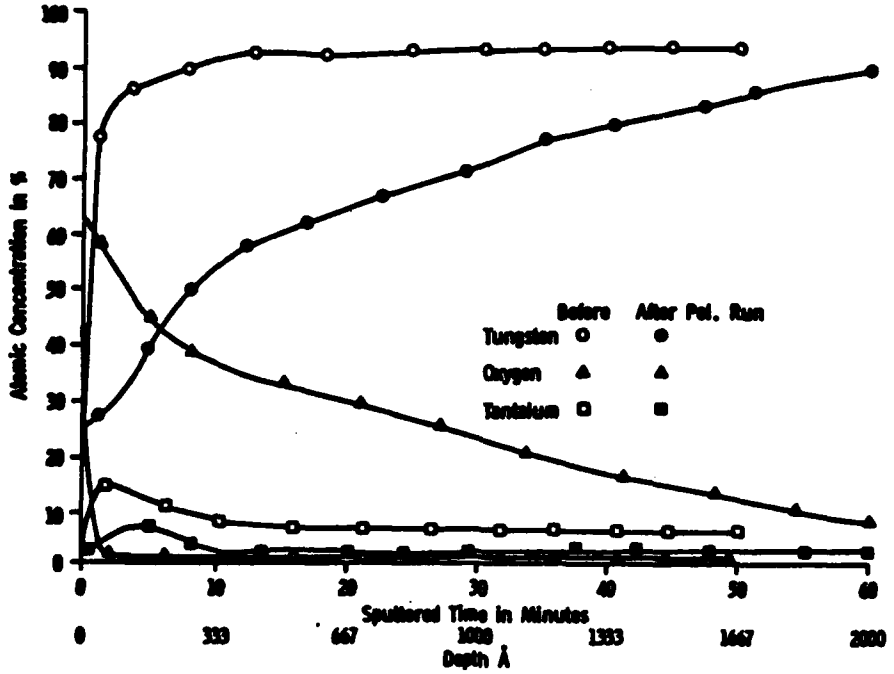

FIGURE 15 — Auger concentration depth profiles of Ta, W, and O *before and after Ta-implanted W2 subjected to potentiodynamic* polarization in pH 9, 0.1 M NaCl solution.

Acknowledgments

The authors acknowledge the assistance of S. Bell in performing the electrochemical experiments.

References

1. J. F. Andrew, M. T. Baker, H. T. Heron, Corrosion and Protection of Sintered Tungsten Alloy Ammunition Components, Proc. 2nd Charlottesville Conf. High Density Materials, October 1980.
2. M. Levy, F. Chang, Corrosion Behavior of High Density Tungsten Alloys, Proc. of the Second International Conference on Environmental Degradation of Engineering Materials in Aggressive Environments, September 21-23, 1981, pp. 33-42.
3. B. E. Wilde, "On Pitting and Protection Potentials: Their Use and Possible Misuses for Predicting Localized Corrosion Resistance of Stainless Alloys in Halide Media," Localized Corrosion, R. W. Staehle, B. F. Brown, J. Kruger, A. Agrawal, Eds., National Association of Corrosion Engineers, Houston, Texas, p. 342, 1974.
4. W. D. France, Jr., Crevice Corrosion of Metals, ASTM STP 516, Localized Corrosion—Cause of Metal Failures, ASTM, Philadelphia, Pennsylvania, pp. 170-171, 1968.
5. M. Pourbaix, Atlas of Electrochemical Equilibria in Aqueous Solutions, National Association of Corrosion Engineers, Houston, Texas, 1974.

DISTRIBUTION LIST

No. of Copies	To
1	Office of the Under Secretary of Defense for Research and Engineering, The Pentagon, Washington, DC 20301
	Commander, U.S. Army Laboratory Command, 2800 Powder Mill Road, Adelphi, MD 20783-1145
1	ATTN: SLCIS-IM-TL
	Commander, Defense Technical Information Center, Cameron Station, Building 5, 5010 Duke Street, Alexandria, VA 22304-6145
2	ATTN: DTIC-FDAC
1	Metals and Ceramics Information Center, Battelle Columbus Laboratories, 505 King Avenue, Columbus, OH 43201
	Commander, Army Research Office, P.O. Box 12211, Research Triangle Park, NC 27709-2211
1	ATTN: Information Processing Office
	Commander, U.S. Army Materiel Command, 5001 Eisenhower Avenue, Alexandria, VA 22333
1	ATTN: AMCLD
	Commander, U.S. Army Materiel Systems Analysis Activity, Aberdeen Proving Ground, MD 21005
1	ATTN: AMXSY-MP, H. Cohen
	Commander, U.S. Army Missile Command, Redstone Scientific Information Center, Redstone Arsenal, AL 35898-5241
1	ATTN: Technical Library
	Commander, U.S. Army Armament, Munitions and Chemical Command, Dover, NJ 07801
2	ATTN: Technical Library
	Director, U.S. Army Ballistic Research Laboratory, Aberdeen Proving Ground, MD 21005
1	ATTN: AMDAR-TSB-S (STINFO)
	Director, Benet Weapons Laboratory, LCWSL, USA AMCCOM, Watervliet, NY 12189
1	ATTN: AMSMC-LCB-TL
	Commander, U.S. Army Engineer School, Fort Belvoir, VA 22060
1	ATTN: Library
	Naval Research Laboratory, Washington, DC 20375
1	ATTN: Technical Library
1	Mr. B. Sartwell - Code 6675
	Chief of Naval Research, Arlington, VA 22217
1	ATTN: Code 471

No. of Copies	To
	Commander, U.S. Air Force Wright Aeronautical Laboratories, Wright-Patterson Air Force Base, OH 45433
1	ATTN: Technical Library
1	AFWAL/MLC
	National Aeronautics and Space Administration, Marshall Space Flight Center, Huntsville, AL 35812
1	ATTN: R. J. Schwinghammer, EH01, Dir., M&P Lab
	Air Force Armament Laboratory, Eglin Air Force Base, FL 32542
1	ATTN: Technical Library
	Air Force Test and Evaluation Center, Kirtland Air Force Base, NM 87115
1	ATTN: Technical Library
	Naval Air Development Center, Warminister, PA 18974
1	ATTN: Technical Library
	Naval Post Graduate School, Monterey, CA 93948
1	ATTN: Technical Library
	Naval Surface Weapons Center, Dahlgren Laboratory, Dahlgren, VA 22448
1	ATTN: Technical Library
	Naval Weapons Center, China Lake, CA 93555
1	ATTN: Technical Library
	Commander, Rock Island Arsenal, Rock Island, IL 61299
1	ATTN: Technical Labrary
	General Dynamics Corporation, Convair Division, P.O. Box 80877, San Diego, CA 92138
1	ATTN: Research Library, U. J. Sweeney
	Georgia Institute of Technology, Atlanta, GA 30332
1	ATTN: Library
	U.S. Department of Commerce, National Bureau of Standards, Gaithersburg, MD 20899
1	ATTN: Technical Library
1	The Charles Stark Draper Laboratory, 68 Albany Street, Cambridge, MA 02139
	Kennemetal, Inc., P.O. Box 231, Latrobe, PA 15650
1	ATTN: O. W. Nichols
	Director, U.S. Army Materials Technology Laboratory, Watertown, MA 02172-0001
2	ATTN: SLCMT-IML
3	Authors

U.S. Army Materials Technology Laboratory,
Watertown, Massachusetts 02172-0001
THE EFFECT OF ION IMPLANTATION ON THE
CORROSION BEHAVIOR OF A HIGH-DENSITY
SINTERED TUNGSTEN ALLOY - Frank C. Chang,
Milton Levy, and Sin-Shong Lin

Technical Report MTL TR 87-38, August 1987, 12 pp -
illus-table

AD ________________

UNCLASSIFIED
UNLIMITED DISTRIBUTION

Key Words

Corrosion resistance
Tungsten alloys
Density

The effect of Cr, Hf, Ta, and Ti ion implantation at a dose rate of 2 X 10^{17} ions cm^{-2} on the electrochemical corrosion behavior of a high-density sintered tungsten alloy has been investigated in Cl^- -free and Cl^- -containing aqueous solution buffered to pH values of 4, 9, and 12. A three-sweep potentiodynamic polarization technique was used to compare the polarization behavior of unimplanted and implanted surfaces. The surfaces of the ion-implanted tungsten alloy were characterized by Auger electron spectroscopic (AES) analysis.

U.S. Army Materials Technology Laboratory,
Watertown, Massachusetts 02172-0001
THE EFFECT OF ION IMPLANTATION ON THE
CORROSION BEHAVIOR OF A HIGH-DENSITY
SINTERED TUNGSTEN ALLOY - Frank C. Chang,
Milton Levy, and Sin-Shong Lin

Technical Report MTL TR 87-38, August 1987, 12 pp -
illus-table

AD ________________

UNCLASSIFIED
UNLIMITED DISTRIBUTION

Key Words

Corrosion resistance
Tungsten alloys
Density

The effect of Cr, Hf, Ta, and Ti ion implantation at a dose rate of 2 X 10^{17} ions cm^{-2} on the electrochemical corrosion behavior of a high-density sintered tungsten alloy has been investigated in Cl^- -free and Cl^- -containing aqueous solution buffered to pH values of 4, 9, and 12. A three-sweep potentiodynamic polarization technique was used to compare the polarization behavior of unimplanted and implanted surfaces. The surfaces of the ion-implanted tungsten alloy were characterized by Auger electron spectroscopic (AES) analysis.

U.S. Army Materials Technology Laboratory,
Watertown, Massachusetts 02172-0001
THE EFFECT OF ION IMPLANTATION ON THE
CORROSION BEHAVIOR OF A HIGH-DENSITY
SINTERED TUNGSTEN ALLOY - Frank C. Chang,
Milton Levy, and Sin-Shong Lin

Technical Report MTL TR 87-38, August 1987, 12 pp -
illus-table

AD ________________

UNCLASSIFIED
UNLIMITED DISTRIBUTION

Key Words

Corrosion resistance
Tungsten alloys
Density

The effect of Cr, Hf, Ta, and Ti ion implantation at a dose rate of 2 X 10^{17} ions cm^{-2} on the electrochemical corrosion behavior of a high-density sintered tungsten alloy has been investigated in Cl^- -free and Cl^- -containing aqueous solution buffered to pH values of 4, 9, and 12. A three-sweep potentiodynamic polarization technique was used to compare the polarization behavior of unimplanted and implanted surfaces. The surfaces of the ion-implanted tungsten alloy were characterized by Auger electron spectroscopic (AES) analysis.

U.S. Army Materials Technology Laboratory,
Watertown, Massachusetts 02172-0001
THE EFFECT OF ION IMPLANTATION ON THE
CORROSION BEHAVIOR OF A HIGH-DENSITY
SINTERED TUNGSTEN ALLOY - Frank C. Chang,
Milton Levy, and Sin-Shong Lin

Technical Report MTL TR 87-38, August 1987, 12 pp -
illus-table

AD ________________

UNCLASSIFIED
UNLIMITED DISTRIBUTION

Key Words

Corrosion resistance
Tungsten alloys
Density

The effect of Cr, Hf, Ta, and Ti ion implantation at a dose rate of 2 X 10^{17} ions cm^{-2} on the electrochemical corrosion behavior of a high-density sintered tungsten alloy has been investigated in Cl^- -free and Cl^- -containing aqueous solution buffered to pH values of 4, 9, and 12. A three-sweep potentiodynamic polarization technique was used to compare the polarization behavior of unimplanted and implanted surfaces. The surfaces of the ion-implanted tungsten alloy were characterized by Auger electron spectroscopic (AES) analysis.